Published OnlineFirst February 3, 2009; DOI: 10.1158/1535-7163.MCT-08-0669

Dasatinib-induced autophagy is enhanced in combination with temozolomide in glioma

Vanessa Milano, Yuji Piao, Tiffany LaFortune, and John de Groot

Brain Tumor Center, The University of Texas M. D. Anderson Cancer Center, Houston, Texas

Abstract

Glioblastoma is defined by its aggressive invasion, microvascular proliferation, and central necrosis. BMS-354825 (dasatinib) is an ATP-competitive small-molecule inhibitor effective in treating drug-resistant tumors with mutant BCR-ABL, KIT, and epidermal growth factor receptor by blocking tyrosine phosphorylation sites that are critical in tumorigenesis. In studying the action of dasatinib in human glioblastoma, we found that levels of phospho-SRC, AKT, and ribosomal protein S6 were decreased in cell lines treated with low nanomolar concentrations of dasatinib at baseline and following stimulation with epidermal growth factor. Furthermore, an increased sensitivity to dasatinib was noted in glioma cells with functional PTEN. Reduction of invasive potential was observed *in vitro* at concentrations well below the IC_{50} of dasatinib, which was corroborated by immunofluorescence staining showing disruption of paxillin localization to focal adhesions and decreases in focal adhesion kinase autophosphorylation. Cell cycle analysis revealed minimal G_1 arrest but a significant increase in autophagic cell death in glioma cells treated with dasatinib as assessed by acridine orange staining and a concomitant increase in light chain 3 expression and processing. Combination treatment of glioma cells with dasatinib and temozolomide resulted in a significant increase in cell cycle disruption and autophagic cell death. Dasatinib in combination with temozolomide more effectively increased the therapeutic efficacy of temozolomide than when dasatinib was combined with carboplatin or irinotecan. These results strongly support the clinical use of dasatinib in the treatment of glioblastoma and provide a rationale for combination therapy with dasatinib and temozolomide. [Mol Cancer Ther 2009;8(2):394–406]

Received 7/16/08; revised 11/18/08; accepted 12/7/08;

published OnlineFirst 02/03/2009.

Grant support: Flow cytometry analysis was done by the Flow Cytometry and Imaging Core Facility at The University of Texas M. D. Anderson Cancer Center funded by NIH grant 5P30CA016672-29 (PI: John Mendelsohn).

The costs of publication of this article were defrayed in part by the payment of page charges. This article must therefore be hereby marked *advertisement* in accordance with 18 U.S.C. Section 1734 solely to indicate this fact.

Requests for reprints: John de Groot, Brain Tumor Center, The University of Texas M. D. Anderson Cancer Center, 1515 Holcombe Boulevard, Unit 431, Houston, TX 77030. Phone: 713-792-7255; Fax: 713-794-4999. E-mail: jdegroot@mdanderson.org

doi:10.1158/1535-7163.MCT-08-0669

Introduction

Glioblastoma is the most common and malignant astrocytic glioma, carrying the WHO designation of grade IV out of four grades (1, 2). Glioblastoma is histologically defined by its marked vascular proliferation and necrosis and shows high cellularity, mitotic activity, and aggressive invasion into normal brain. Molecularly, these *de novo* neoplasms are characterized by epidermal growth factor (EGF) receptor (EGFR), platelet-derived growth factor receptor, vascular endothelial growth factor receptor, and cyclin-dependent kinase 4 mutations and amplifications; additionally, they exhibit a high frequency of PTEN dysfunction (3). Despite maximal tumor resection, radiation, and chemotherapy, the high degree of infiltration of glioblastoma leads to 100% recurrence and an average life expectancy of only 12 to 14 months (4–6).

BMS-354825 (dasatinib) is an ATP-competitive small-molecule inhibitor effective in combating malignancies characterized by drug-resistant mutants of BCR-ABL, KIT, and EGFR by interfering with aberrantly activated phosphorylation sites (7–10). At low nanomolar concentrations, dasatinib inhibits progression of chronic myelogenous leukemia, pancreatic adenocarcinoma, colon cancer, prostate cancer, non-small cell lung cancer, and breast malignancies (10–15). In glioblastoma, we aimed to target the SRC nonreceptor tyrosine kinase. SRC family kinases include eight homologous members (SRC, YES, FYN, LYN, LCK, HCK, FGR, and BLK) that are implicated in numerous oncogenic pathways (14, 16–18). SRC-type family members exhibit two primary phosphorylation sites: an activating phosphorylation at Tyr^{419} and a deactivating phosphorylation at Tyr^{527} (19, 20). Oncogenesis has been found to occur when inactive and active forms of SRC kinases are in disequilibrium. This imbalance may take place either when SRC itself is mutated or when proteins that regulate SRC, such as the activating agents PTPα and SHP1 and the deactivating agents CSK and CHK, are abnormal or overexpressed (21). Several SRC family members have been shown to be activated in glioblastoma, including the malignant phenotype-promoting members LYN and FYN (22, 23).

SRC mediates many critical proteins that when dysregulated contribute highly to proliferation, invasion, and vasculogenesis through interconnected signaling cascades. These proteins include focal adhesion kinase (FAK), which colocalizes with p130CAS, integrin $\alpha_v\beta_3$, and paxillin to form focal adhesions, and AKT, which is a downstream effector of the phosphatidylinositol 3-kinase (PI3K) pathway

Published OnlineFirst February 3, 2009; DOI: 10.1158/1535-7163.MCT-08-0669

(24–28). In addition, SRC appears to activate the mitogen-activated protein kinase (p44/42 MAPK) in cooperation with Grb2/PI3K regulation via activation by platelet-derived growth factor receptor, ultimately instigating tumorigenic transcription and gene expression (29, 30).

We studied dasatinib as a known inhibitor of SRC activation in glioblastoma with emphasis on inhibiting the SRC-activating phosphorylation at Tyr^{419}, a site that has been implicated in the autophosphorylation of FAK at Tyr^{397} (28). We show the inhibitory effect of dasatinib on tumor proliferation in multiple glioma cell lines via the blockage of SRC, AKT, and ribosomal protein S6 (rpS6) activation. Dasatinib also inhibited glioma invasion in a Matrigel invasion assay by preventing FAK autophosphorylation and focal adhesion formation. Furthermore, we show that dasatinib has the capacity to initiate type II (autophagic) programmed cell death without inducing apoptosis. Finally, we show that dasatinib and temozolomide combine synergistically in the inhibition of cell proliferation.

Materials and Methods

Cell Lines and Culture Conditions

To assess the effect of dasatinib in human gliomas, we used the LN18, U251, U87/EGFR (U87 cells stably expressing wild-type EGFR), and U87/EGFR PTEN (U87 cells stably expressing both wild-type EGFR and functional PTEN; both U87 cell lines were a generous gift of Dr. Paul Mischel, University of California at Los Angeles) human glioblastoma cell lines. The LN18 cell line with stable lentiviral vector-mediated knockdown of PTEN (LN18 shPTEN) was a gift from Dr. Ta-Jen Liu (The University of Texas M. D. Anderson Cancer Center). All cell lines were maintained as monolayer cultures in DMEM/F-12 supplemented with 10% fetal bovine serum (Life Technologies) and 1.0% penicillin/streptomycin and were incubated in an environment of 10% CO_2/90% air at 37°C.

Reagents

Dasatinib was dissolved in DMSO (Sigma) to a concentration of 20 mmol/L. The solution was stored at −20°C and further diluted as needed to an appropriate final concentration in serum-containing DMEM/F-12 (Life Technologies). Chemotherapeutic sources: temozolomide (Schering-Plough), irinotecan (Pharmacia & Upjohn), and carboplatin (Sigma). 3-Methyladenine (3-MA; Sigma), an inhibitor of autophagosome formation, was dissolved in medium containing 10% fetal bovine serum.

Cell Proliferation Assay

The antiproliferative activity of dasatinib on cells growing in culture was quantified using a sulforhodamine B (SRB)-based assay (31). Cells were seeded into 96-well plates at 3×10^3 per well and allowed to adhere overnight in medium containing 10% fetal bovine serum. The cells were maintained in standard culture conditions after treatment with dasatinib, and cell growth was measured by fixing the cells with 10% TCA and subsequent staining with SRB. The wells were read at 530 and 620 nm using spectrophotometric analysis. Drug interactions were determined using the CalcuSyn Software (Biosoft). This program uses the median effect equation to determine the median dose effect, Dm, which is analogous to the IC_{50}. Synergy or antagonism [quantified by the combination index (CI)] is based on the multiple drug effect equation where CI = 1 indicates an additive effect, CI < 1 indicates synergy, and CI > 1 implies antagonism (32).

Matrigel Invasion Assay

Invasion of glioma cells *in vitro* was measured by the invasion of cells through Matrigel-coated 24-well Transwell inserts. Cells (1×10^6) were treated with 50, 100, and 200 nmol/L dasatinib for 24 h in 10-cm plates and washed with serum-free medium. Cells (2.5×10^5) were then transferred to each Transwell in duplicate, and the cells were allowed to invade for 24 h at 37°C. Invading cells were stained with 0.1% crystal violet in methanol and quantified by dissolving the Transwell inserts in a 2.0% sodium deoxycholate solution, which was subsequently analyzed spectrophotometrically at 595 nm.

Immunofluorescence Staining

U251, U87/EGFR, and LN18 cells were plated on glass slides in 6-well culture plates at a concentration of 2×10^5 per well for 24 h and subsequently treated with dasatinib for an additional 24 h. Thereafter, the cells were fixed with a 3.7% formaldehyde solution in PBS and then permeabilized with 1.0% Triton X-100 in PBS. Paxillin was visualized by incubating first with mouse anti-paxillin monoclonal antibody (BD Biosciences) and then with Texas red-conjugated goat antibody to mouse IgG (Invitrogen). Actin filaments were stained with phalloidin conjugated with Alexa Fluor 488 (Invitrogen). Nuclei were stained with 5.0 ng/mL Hoechst 33258 for 15 min at room temperature. Pictures were taken under a Zeiss Axioskop 40 microscope equipped with the appropriate filters and aid of AxioVision 4.4 software.

Western Blotting Analysis

To determine dasatinib-mediated cell signal changes, we evaluated the effect of dasatinib on phosphorylation of SRC, FAK, MAPK, AKT, and rpS6 in U251 human glioma cells. Cells were plated onto 10-cm plates at a concentration of 2×10^6 and then incubated for 24 h. The next day, cells were treated for the indicated length of time with varying concentrations of dasatinib diluted in fresh DMEM. To assess the activity of dasatinib in cell lines with and without expression of the tumor suppressor PTEN, the effect of dasatinib was evaluated in the context of inhibiting EGF-stimulated tyrosine phosphorylation of EGFR, SRC, FAK, MAPK, AKT, and rpS6. Cells (2×10^6) were seeded onto 10-cm plates in DMEM, serum starved for 24 h, and then treated with various concentrations of dasatinib in serum-free medium for 8 h. The cells were further treated with 50 ng/mL human recombinant EGF (Upstate Biotechnology) for 15 min. Protein (30 μg) was electrophoresed on a 10% SDS-PAGE gel and transferred to an Immuno-Blot polyvinylidene difluoride membrane (Bio-Rad). Membranes were then probed with primary antibodies: phospho-EGFR (Tyr^{1173}), phospho-SRC (Tyr^{419}), phospho-SRC

Published OnlineFirst February 3, 2009; DOI: 10.1158/1535-7163.MCT-08-0669

(Tyr^{527}), phospho-MAPK (Thr^{202}/Tyr^{204}), total MAPK, phospho-AKT (Thr^{308}, Ser^{473}), total AKT, and phospho-S6 (Ser^{235}/Ser^{236}, Ser^{240}/Ser^{244}; Cell Signaling); PTEN, total SRC, and total FAK (Santa Cruz Biotechnology); phospho-FAK (Tyr^{397}; Zymed Invitrogen); EGFR Ab4 (Calbiochem); and β-actin (Sigma-Aldrich).

Cell Cycle Analysis

Glioma cells were plated at a density of 5×10^5 per well in 10-cm plates and maintained in 10% fetal bovine serum medium overnight. The following day, the cells were treated with varying concentrations of dasatinib and temozolomide in 10% DMEM for the indicated length of time. Cells were harvested, washed with 1× PBS, and suspended in 100% ethanol at −20°C overnight. Cells were spun out of fix at 1,500 rpm for 5 min, and the pellets were stained with 1× propidium iodide and followed by treatment with 7 μg/mL RNase A. DNA content was then analyzed on a FACScan flow cytometer.

Apoptosis Assays

Apoptosis was quantified using the Annexin V-FLUOS Apoptosis kit (Roche) according to the manufacturer's instructions. Treated U87/EGFR, LN18, and U251 glioma cells were incubated in standard culture conditions with and without drug treatment for 72 h before staining and subsequent flow cytometric analysis. We also analyzed cells for evidence of apoptosis using a terminal deoxynucleotidyl transferase-mediated dUTP nick-end labeling kit per the manufacturer's instructions (Calbiochem).

Detection of Autophagy with Acridine Orange Staining and Light Chain 3 Epifluorescence

To detect the formation of acidic vesicular organelles, cells were treated and then stained with 1.0 μg/mL acridine orange for 15 min. Cells were then trypsinized, collected in PBS, and analyzed using the FACScan flow cytometer.

U87 and U251 cells were transfected with a GFP-light chain 3 (LC3) vector (in pEGFP-C1) kindly provided by Dr. Oliver Bogler (The University of Texas M. D. Anderson Cancer Center) using the FuGENE 6 transfection reagent (Roche) according to the manufacturer's instructions. At 48 h, cells were plated on glass slides and treated with drug. After exposure to temozolomide, dasatinib, or the combination of these agents for 72 h, cells were fixed in 1% paraformaldehyde and analyzed by fluorescence microscopy.

Statistical Analysis

Mean and SD were calculated for the biological effect of dasatinib in the different assays. Statistical significance between groups was compared using the Student's *t* test. One-sided tests were considered significant at a level of 0.05. All data were analyzed using the GraphPad Instat3 software (GraphPad Software).

Results

Treatment with Dasatinib Inhibits Glioma Cell Growth *In vitro*

The ability of dasatinib to inhibit glioma cell proliferation *in vitro* was evaluated with the aid of a SRB assay (31). LN18, U251, and U87/EGFR cells were treated with a wide range of dasatinib concentrations (0, 1.0, 10, 100, 500, and 1,000 nmol/L) to capture its IC_{50} of antitumor activity. Cell viability was assessed after 72 h, and the results of SRB staining are shown (Fig. 1A). Dasatinib showed significant ($P < 0.05$) antiproliferative activity at low nanomolar concentrations in U251 and LN18 glioma cells, yielding an IC_{50} at 210 and 420 nmol/L, respectively. U87 cells stably expressing wild-type EGFR were found to be more resistant to dasatinib and exhibited an IC_{50} of 1.5 μmol/L.

To explore the mechanisms mediating the growth-inhibitory effect of dasatinib, we tested its ability to inhibit kinases important in mitogenic signaling and survival pathways, including SRC, p44/42 MAPK, AKT, and rpS6. U251 was selected as a representative cell line due to its IC_{50} and mutant p53 and PTEN-deficient status. Cells were treated with 200 nmol/L dasatinib for 2, 4, 8, 24, and 48 h. Attached and floating cells were collected for protein and Western blotting analysis (Fig. 1B) and revealed a decrease in SRC Y419 phosphorylation at 8 h. After an initial decrease, there was a time-dependent increase in SRC Y527 phosphorylation reflecting an accumulation of SRC protein with phosphorylation of its negative regulatory tyrosine residue (33). Slight decreases in both serine and threonine phosphorylation of AKT were seen as early as 2 h, an effect that became more apparent by 8 h. Phosphorylation of the AKT Thr^{308} residue, however, exhibited some reactivation at 24 and 48 h, whereas Ser^{473} phosphorylation was not reinstated but did not reach the same level of attenuation as threonine phosphorylation. Similarly, phosphorylation of S6 was decreased by dasatinib treatment, with Ser^{235}/Ser^{236} showing a more rapid response and subsequent recovery at 48 h, whereas Ser^{240}/Ser^{244} phosphorylation declined more slowly but was sustained. The inhibition of S6 phosphorylation is important as a downstream indicator of transcriptional inhibition. In contrast to SRC, AKT, and S6, the phosphorylation of p44/42 MAPK showed an increase over the course of 24 h.

Expression of PTEN in Glioma Cells Affects Sensitivity to Dasatinib

We further pursued a possible link between PTEN expression and sensitivity to dasatinib by analyzing the expression of endogenous PTEN in U251 and the syngeneic cell line pairs of U87/EGFR and U87/EGFR PTEN (courtesy of Dr. Paul Mischel; characterized previously; ref. 34) and LN18 and LN18 shPTEN. The Western blot shown in Fig. 2A shows a moderate and high level of PTEN expression in LN18 and U87/EGFR PTEN, respectively, compared with the diminished PTEN levels in LN18 shPTEN, U251, and U87/EGFR cells. With these data, it is possible to make a preliminary association between the PTEN status of a cell line and the effect of dasatinib (Fig. 2B). LN18, with an IC_{25} of 22 nmol/L and an IC_{50} of 420 nmol/L, is more sensitive to dasatinib in comparison with LN18 shPTEN, which was 3- to 5-fold more resistant with IC_{25} and IC_{50} values of 100 nmol/L and >1.5 μmol/L, respectively. The PTEN-negative U251 is less resistant than LN18, exhibiting an IC_{25} of 9 nmol/L and an IC_{50} of

Published OnlineFirst February 3, 2009; DOI: 10.1158/1535-7163.MCT-08-0669

210 nmol/L (Fig. 1A). U87/EGFR, the more resistant PTEN-negative cell line studied, displayed an IC_{25} of 62 nmol/L and an IC_{50} of 1.5 μmol/L. U87/EGFR became >2.5- to 8-fold more sensitive to dasatinib when PTEN was reintroduced (IC_{25}, 24 nmol/L; IC_{50}, 180 nmol/L) compared with U87/EGFR. The disparity of dasatinib sensitivity between U87/EGFR and U251 may be explained by the abundance of EGFR in the former cell line and genetic heterogeneity and may consequently not be a reflection of PTEN levels alone.

To determine whether mitogenic signaling via AKT was affected by PTEN expression status, we stimulated U87/EGFR and U87/EGFR PTEN cells with human recombinant EGF. A dose slightly lower than each cell line's respective IC_{50} was used during the treatment phase: 1.0 μmol/L for U87/EGFR and 100 nmol/L for U87/EGFR PTEN. Western blotting (Fig. 2C) shows that dasatinib was able to maintain an inhibitory effect vis-à-vis AKT phosphorylation and transcription-activating rpS6 phosphorylation at Ser^{240}/Ser^{244} (but not Ser^{235}/Ser^{236}) in serum-free medium and when EGFR was activated. Additionally, the same inhibitory effect was achieved with lower concentrations of dasatinib in PTEN-containing cells (U87/EGFR PTEN) as in PTEN-deficient cells (U87/EGFR PTEN) treated with a higher dose. Western blot analysis was done three times with similar results.

Glioma Cell Transwell Migration Is Abrogated by Dasatinib Treatment

To determine the effect of dasatinib-induced SRC inhibition on glioma migration, we conducted a Matrigel Transwell migration assay. LN18 and U251 cells were treated with 0, 50, 100, and 200 nmol/L dasatinib for 24 h in serum-containing medium before being allowed to invade through Matrigel-coated membranes in serum-free medium. No change in cell viability was seen following 24 h treatment with dasatinib according to a previously conducted SRB assay. Dasatinib suppressed the migration of glioma cells across the Matrigel-coated Transwells: quantification of the stained membranes exposes a dose-dependent decrease in invasion that begins at treatment with 50 nmol/L dasatinib. Indeed, a ~50% decrease in invasion was observed at 50 nmol/L in both cell lines, with LN18 being slightly less sensitive (Fig. 3A).

Because SRC affects autophosphorylation of FAK at Tyr^{397}, promoting the localization of FAK, paxillin, and $\alpha_v\beta_3$ integrin to focal adhesions, immunofluorescence of paxillin was carried out to visualize the extent of focal adhesion formation in U251 glioma cells treated with 200 nmol/L dasatinib. Untreated cells (Fig. 3B) displayed focal adhesions staining positive for both actin and paxillin. Treatment with dasatinib significantly diminished the presence of these podia, and paxillin was observed to be diffuse throughout the cytoplasm; additionally, the dasatinib-treated cells adopted a more elongated morphology. Quantification of focal adhesions in untreated and treated U251 and LN18 cells (Fig. 3C) further underscores the extent of focal adhesion disruption in glioma cells.

In addition to SRC, which plays an important role in migration and invasion, activation of FAK Y397 is also integral to focal adhesion formation and cellular movement. LN18 and U251 glioma cells were treated with dasatinib for 24 h and cell lysate was obtained and

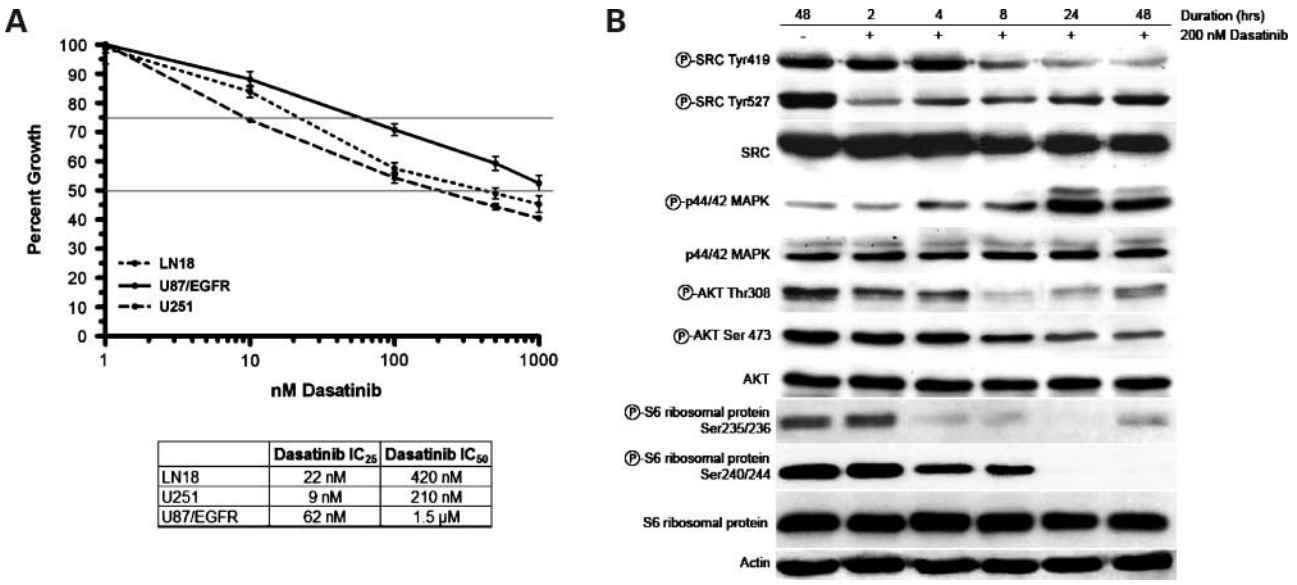

	Dasatinib IC_{25}	Dasatinib IC_{50}
LN18	22 nM	420 nM
U251	9 nM	210 nM
U87/EGFR	62 nM	1.5 μM

Figure 1. Dasatinib treatment exhibits an inhibitory effect on glioma proliferation. **A,** glioma cells were seeded at a density of 3×10^6 in a 96-well culture late. Serum-free medium containing 0, 1.0, 10, 100, 500, and 1,000 nmol/L dasatinib was added to the wells in triplicate. After 72 h, viable cells were stained with SRB and quantified using a spectrophotometer. *Points,* mean of triplicate determinations from two independent experiments; *bars,* SD. **B,** U251 cells were plated at a concentration of 1×10^6 before being treated with 200 nmol/L dasatinib in 10% medium. Phosphorylation of AKT, rpS6, SRC (Y419 and Y527), and p44/42 MAPK activation was assessed by Western blot. A decrease in the activation of SRC was accompanied by a decrease in c-SRC levels. β-Actin was employed as a loading control. Representative of three independent experiments.

Published OnlineFirst February 3, 2009; DOI: 10.1158/1535-7163.MCT-08-0669

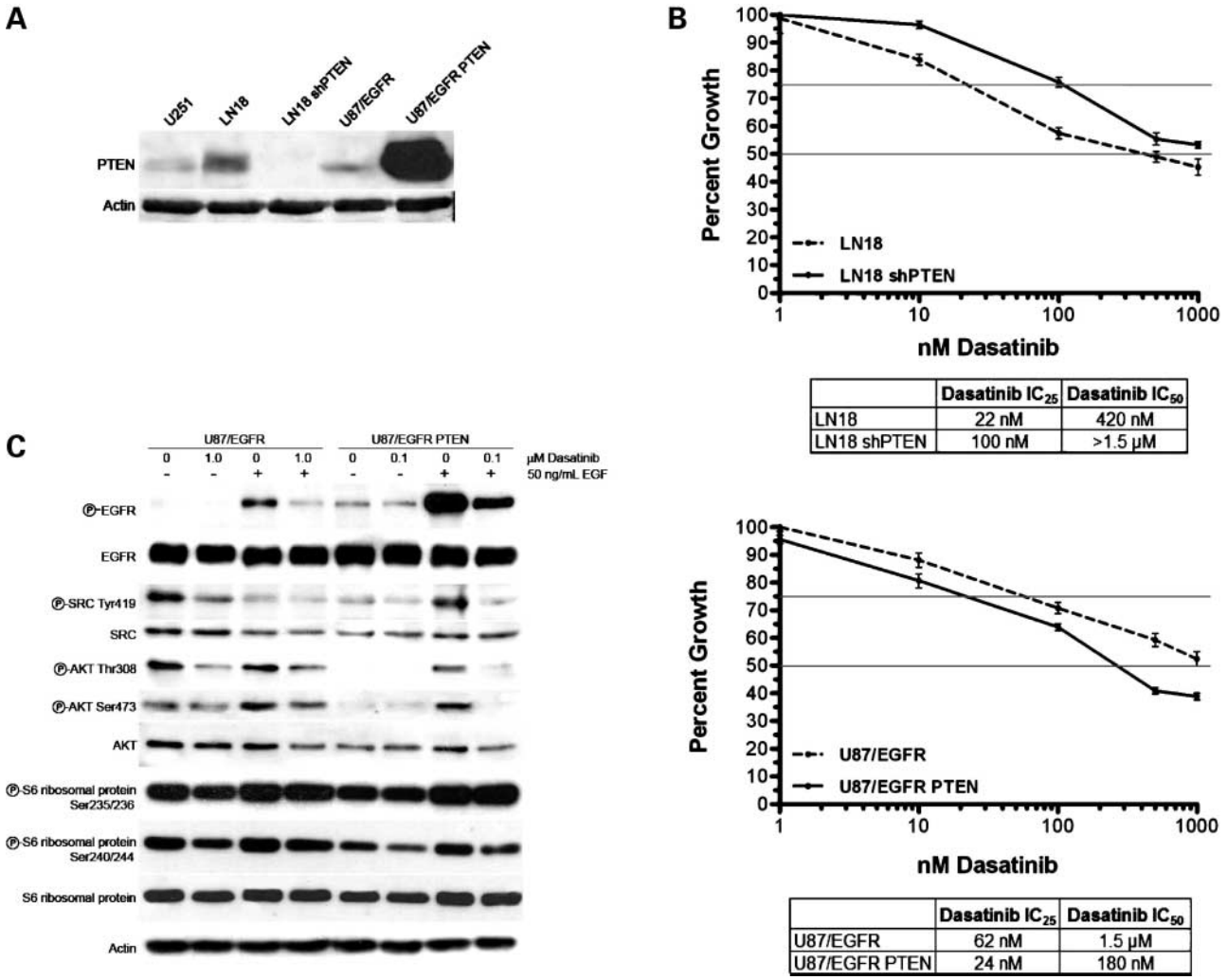

Figure 2. PTEN levels influence sensitivity of cells to dasatinib. **A,** syngeneic glioma cell lines (U87/EGFR and U87/EGFR PTEN; LN18 and LN18 shPTEN) were assessed for the level of PTEN expression. Cells were allowed to adhere in 10% serum-free medium for 48 h and subsequently collected for Western blot analysis. **B,** transfection of PTEN affects sensitivity of glioma cells to dasatinib in a 72 h SRB growth assay. The dose needed to achieve a 25% (IC_{25}) and 50% (IC_{50}) effect was lower in cells stably expressing PTEN than in PTEN-deficient cells. Alternatively, LN18 cells with knockdown of PTEN had 3-fold decrease sensitivity to the effects of dasatinib compared with parental control cells. *Points,* average of three determinations from three independent experiments. **C,** U87/EGFR and U87/EGFR PTEN glioma cells were serum depleted for 24 h before they were treated with the IC_{50} of dasatinib. Following 8 h of treatment in serum-free medium, cells were stimulated with 50 ng/mL EGF for 15 min. Representative of three independent experiments.

analyzed by Western blotting. Figure 3D displays a dose-dependent decrease in FAK autophosphorylation beginning at 100 nmol/L in both cell lines. As suggested by the invasion assay, LN18 cells displayed more persistent FAK phosphorylation than U251 cells. In these glioma cells, inhibition of Transwell migration appears to be mediated to a large extent by inhibition of SRC, further augmented at higher dasatinib concentrations by concurrent inhibition of FAK.

Dasatinib Does Not Induce G_1 Arrest or Apoptosis in Glioma

Because dasatinib was found to be effective against cell proliferation, we appraised the effect of dasatinib on the cell cycle (Fig. 4A). U87/EGFR and LN18 cells were treated with 0, 100, 200, and 500 nmol/L dasatinib for 24, 48, and 72 h. Fluorescence-activated cell sorting analysis showed minimal increase in the proportion of cells in the G_1 phase at 72 h (<10%), and the G_2-M- and S-phase cell numbers were similar between treated and untreated cells (see Supplementary Fig. S1 for tabulated results).[1]

Temozolomide is an alkylating agent used as the standard-of-care treatment of glioblastoma and is known to induce G_2 cell cycle arrest. To examine the effect of combining dasatinib with temozolomide, we performed fluorescence-activated cell sorting analysis on LN18, U251,

[1] Supplementary material for this article is available at Molecular Cancer Therapeutics Online (http://mct.aacrjournals.org/).

Published OnlineFirst February 3, 2009; DOI: 10.1158/1535-7163.MCT-08-0669

and U87/EGFR cell lines treated for 24, 48, and 72 h with 200 nmol/L dasatinib and the varying concentrations of temozolomide to examine the extent of G_1 and G_2-M cell cycle change. Figure 4B shows that dasatinib induced minimal G_1 accumulation but temozolomide monotherapy induced a significant G_2-M arrest. The combination-treated cells exhibited a more equal accumulation in both G_1 and G_2-M. Additionally, a negligible decrease in the S-phase

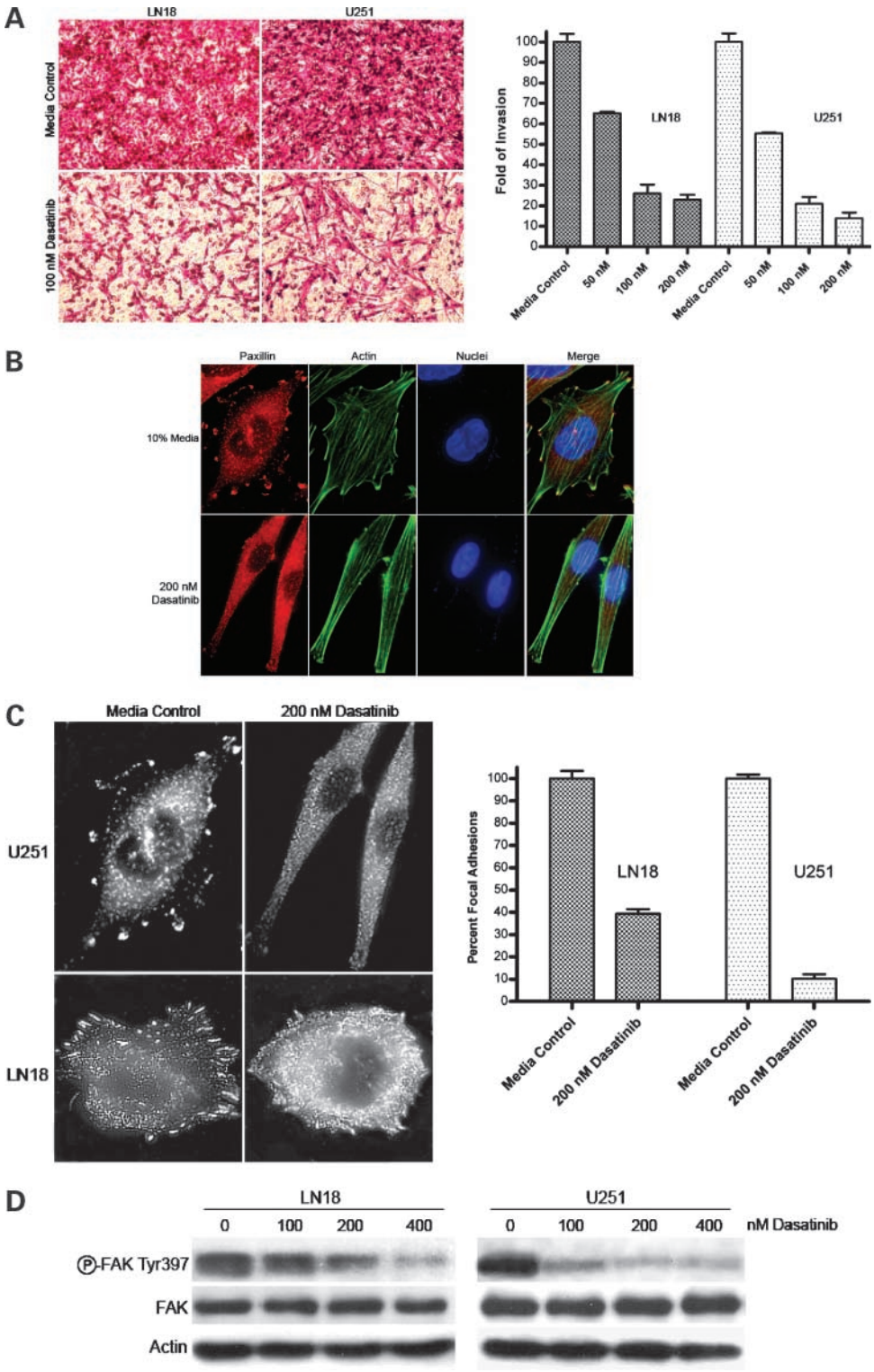

Figure 3. Treatment with dasatinib inhibits glioma invasion and focal adhesion formation. **A,** LN18 and U251 glioma cells were treated with 0, 50, 100, and 200 nmol/L dasatinib in serum-free medium. After 24 h, the cells were counted and 2.5×10^5 viable cells in serum-free medium were added to inserts precoated with Matrigel in duplicate. Invasion took place in standard culture conditions for a period of 24 h. Representative images (×20) of the bottom insert surface exhibit crystal violet-stained invading cells, which can be readily distinguished from the membrane pores and surface. To quantify the effect of dasatinib on invading glioblastoma cells, crystal violet-stained Matrigel membranes were dissolved in 2.0% deoxycholate and the absorbance was then measured using a spectrophotometer. *Points,* mean of triplicate determinations from three independent experiments; *bars,* SD. Quantification showed a significant decrease in invasion at low nanomolar concentrations of dasatinib in both cell lines ($P < 0.05$). **B,** immunofluorescence of U251 cells was done following 24 h of treatment with 200 nmol/L dasatinib. Distribution of paxillin within focal adhesions and cytosol was visualized using primary anti-paxillin and secondary Texas red-conjugated goat anti-mouse antibodies. Filamentous actin structure was discerned by staining with Alexa Fluor 488-conjugated phalloidin, and nuclei were stained with Hoechst 33258. Dasatinib-treated cells displayed greater perinuclear localization of paxillin, less focal adhesions, and a more elongated morphology. **C,** glioma cells were treated with dasatinib and stained as described previously. The prevalence of focal adhesions after treatment was quantified by scoring the incidence of clustered paxillin staining of 100 cells from three separate experiments. As shown, focal adhesion presence is diminished by dasatinib in U251 and LN18 cells. **D,** U251 and LN18 glioma cells were seeded onto 10-cm plates and treated with 0, 100, 200, and 400 nmol/L dasatinib in serum-containing medium. Cell lysates were collected after 24 h and analyzed for the expression of autophosphorylated FAK Y397 and total FAK. Treatment with dasatinib affected a dose-dependent decrease in FAK activation in both cell lines. Western blots were repeated three times with similar results.

Published OnlineFirst February 3, 2009; DOI: 10.1158/1535-7163.MCT-08-0669

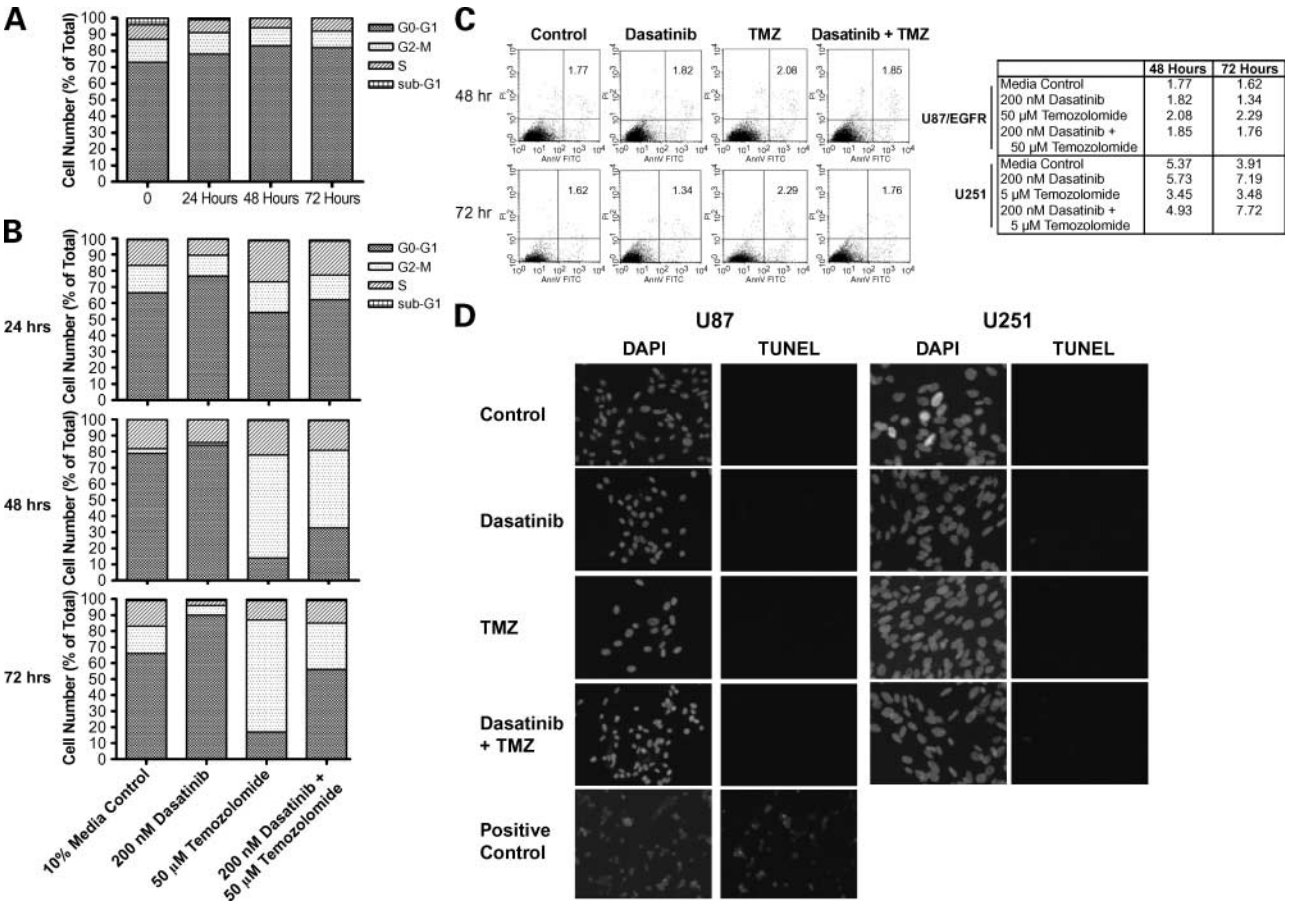

	48 Hours	72 Hours
Media Control	1.77	1.62
200 nM Dasatinib	1.82	1.34
50 μM Temozolomide	2.08	2.29
200 nM Dasatinib + 50 μM Temozolomide	1.85	1.76
Media Control	5.37	3.91
200 nM Dasatinib	5.73	7.19
5 μM Temozolomide	3.45	3.48
200 nM Dasatinib + 5 μM Temozolomide	4.93	7.72

Figure 4. Treatment with dasatinib affects G_1 status in glioma cells. **A,** cell cycle analysis was done on U87/EGFR glioma cells treated with 250 nmol/L dasatinib for 0, 24, 48, and 72 h. Cell cycle data represent a population of 10,000 cells analyzed on a FACScan cytometer in triplicate. Representative data for U87/EGFR cells highlights minimal G_1 arrest (<10%) in U87/EGFR cells treated with 250 nmol/L dasatinib. **B,** cell cycle analysis was done on U87/EGFR cells treated for 24, 48, and 72 h with dasatinib and temozolomide alone and in combination. Dasatinib alone had minimal effects on G_1, temozolomide alone induced G_2 arrest, whereas both G_1 and G_2 arrest was seen when the two treatments were combined. **C,** representative flow cytometric analysis following Annexin V staining of U87/EGFR cells treated for 48 and 72 h with dasatinib (200 nmol/L), temozolomide (50 μmol/L), or the combination from three independent experiments. A lack of significant induction of apoptosis was also observed in U251 cells (*right*). **D,** U87/EGFR and U251 cells treated with dasatinib (200 nmol/L), temozolomide (50 μmol/L), or the combination did not show positive terminal deoxynucleotidyl transferase-mediated dUTP nick-end labeling staining at 72 h. Terminal deoxynucleotidyl transferase-mediated dUTP nick-end labeling staining was repeated twice with identical results.

population was apparent. Little to no sub-G_1 cells were present compared with the total cell number.

Because little or no increase in the sub-G_1 cell fraction was observed, we evaluated the effect of these agents alone and in combination on the induction of apoptosis. A lack of apoptosis was confirmed by the absence of Annexin V staining (Fig. 4C), which was corroborated by a lack of terminal deoxynucleotidyl transferase-mediated dUTP nick-end labeling positivity in treated cells (Fig. 4D). This prompted the notion that dasatinib may trigger cell death by an alternate mechanism such as autophagy.

Augmentation of Dasatinib-Induced Autophagy in Combination with Temozolomide

Considering the absence of apoptotic cell populations, we evaluated the ability of dasatinib to induce autophagic cell death. In addition, as temozolomide also induces autophagy (35), we studied these agents in combination to determine whether this possibly shared mechanism of action resulted in synergistic antitumor activity. U87/EGFR and U251 cells were treated with 200 nmol/L dasatinib and 50 and 5 μmol/L temozolomide, respectively, for 48 and 72 h. Following treatment, the cells were stained with 1.0 mg/mL acridine orange, which detects the formation of acidic cellular vesicles, a hallmark of autophagy (but not exclusively so; refs. 35, 36; Fig. 5A). U87/EGFR cells showed an increased percentage of cells stained with acridine orange when treated for 48 h with 200 nmol/L dasatinib and 50 μmol/L temozolomide as monotherapies; this effect was intensified when the two drugs were used in tandem. However, U87/EGFR cells were not as sensitive as U251 cells, which displayed approximately twice as much response when treated with dasatinib alone. This may be because the IC_{50} of dasatinib for U251 is much lower than that of U87/EGFR. Additionally, U87/EGFR cells were

Published OnlineFirst February 3, 2009; DOI: 10.1158/1535-7163.MCT-08-0669

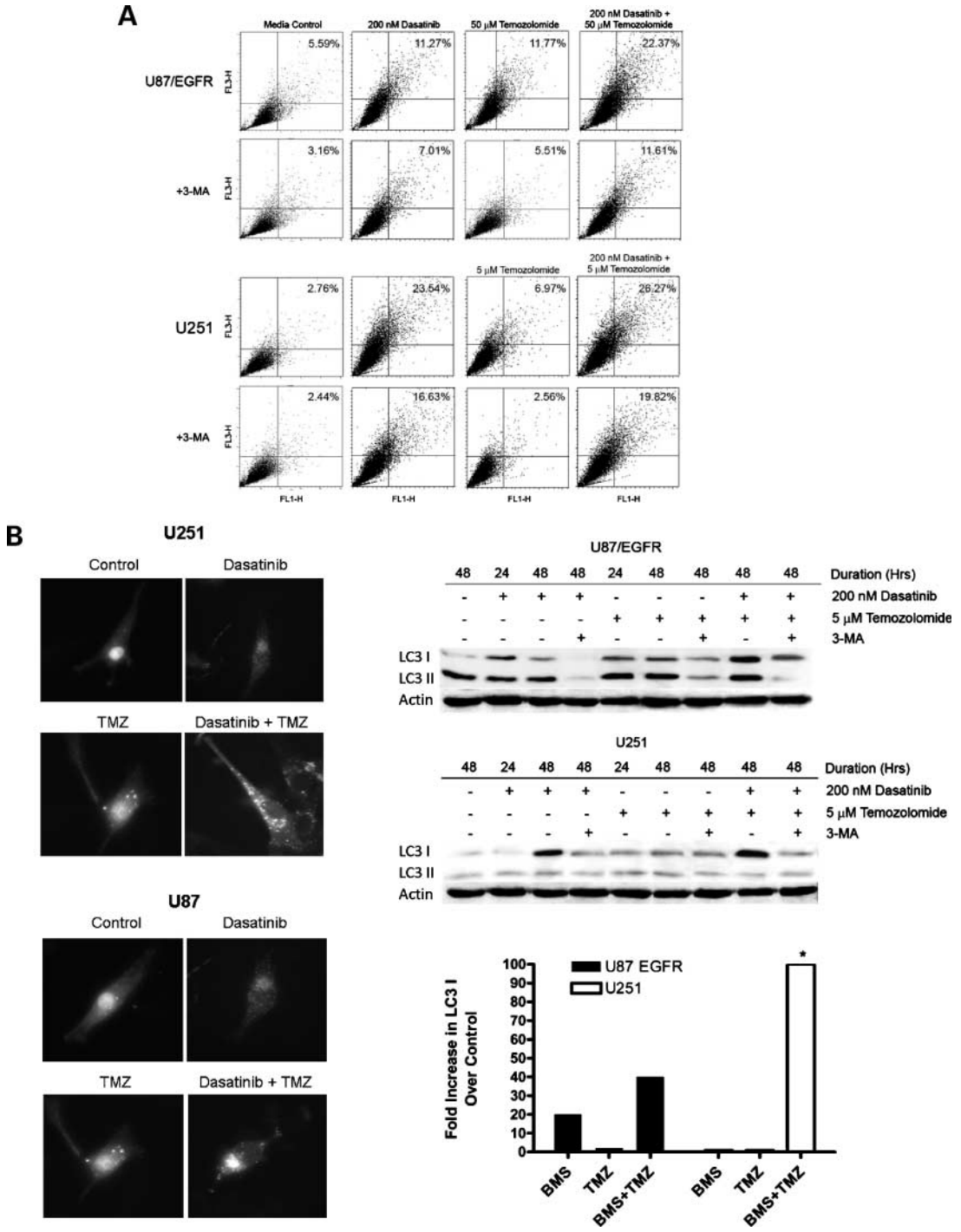

Figure 5. Combination treatment of glioma cells with dasatinib and temozolomide exhibits a significant decrease in cell proliferation while simultaneously increasing autophagy. **A,** autophagic cell death was analyzed in U251 and U87/EGFR cells treated for 48 h with the combination temozolomide IC_{50} and 200 nmol/L dasatinib by staining with 1.0 mg/mL acridine orange. The differential staining of acridine orange can detect the acidic vesicles of autophagic cells (*top right* and *left quadrants*). As shown, dasatinib increases autophagy in glioma cells, an effect that is amplified by temozolomide. 3-MA (2 mmol/L), added 24 h after the start of dasatinib and temozolomide treatment, was used to successfully reverse the autophagic effect. FL1-H indicates green color intensity and FL3-H shows red color intensity. Results were confirmed in three separate experiments. **B,** punctate signal of GFP-LC3 in dasatinib cells becomes more dramatic in cells treated with both dasatinib and temozolomide (*left*). The expression of LC3, an autophagic marker, was examined in cells treated with dasatinib and temozolomide. Treatment with dasatinib increased protein expression of LC3-I at 48 h, and combination treatment with temozolomide further augmented LC3 protein expression (*right*). Temozolomide only affected a LC3-I increase in U87/EGFR cells as was suggested by the previous acridine orange staining. LC3-I and -II expression was reduced by 3-MA in dasatinib- and temozolomide-treated cells. Densitometry confirms the synergistic increase in LC3-I expression (*asterisk,* >100% increase over baseline). Western blots were repeated thrice.

Published OnlineFirst February 3, 2009; DOI: 10.1158/1535-7163.MCT-08-0669

C

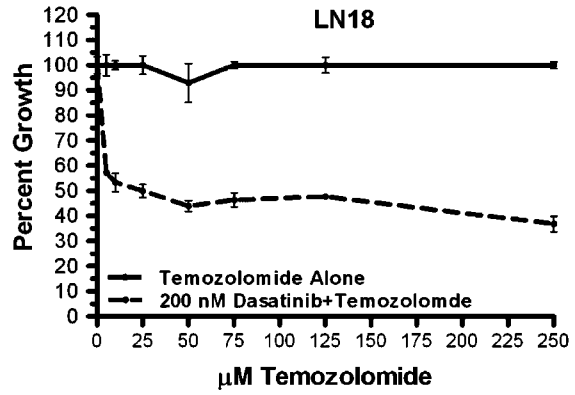

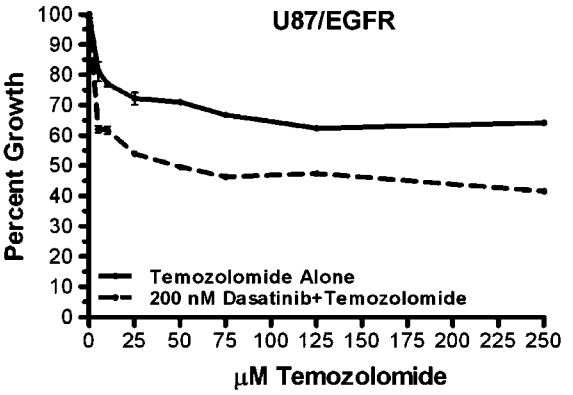

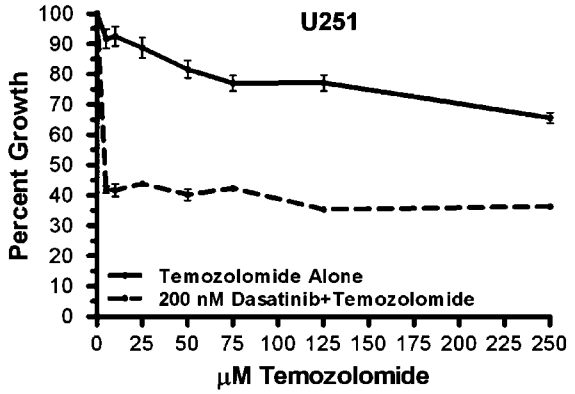

	Dasatinib Dose	Temozolomide Monotherapy IC_{50}	New Temozolomide IC_{50}	Combination Index
LN18	200 nM	No Effect	25 μM	0.935
U87/EGFR	200 nM	3050 μM	50 μM	0.135
U251	200 nM	1860 μM	<5.00 μM	<0.292

Combination Index (CI) Values

	LN18	U87/EGFR	U251
200 nM Dasatinib + 5 μM Temozolomide	1.809	0.758	0.292
200 nM Dasatinib + 10 μM Temozolomide	1.266	0.744	0.285
200 nM Dasatinib + 25 μM Temozolomide	0.935	0.238	0.383
200 nM Dasatinib + 50 μM Temozolomide	0.546	0.135	0.252
200 nM Dasatinib + 75 μM Temozolomide	0.681	0.089	0.339
200 nM Dasatinib + 125 μM Temozolomide	0.762	0.124	0.15
200 nM Dasatinib + 250 μM Temozolomide	0.282	0.067	0.202

D

	U87/EGFR	U251
Dasatinib Dose	200 nM	200 nM
Carboplatin Monotherapy IC_{50}	6.76 μM	15.06 μM
Combination Carboplatin IC_{50}	3.89 μM	9.21 μM
Carboplatin CI at IC_{50}	0.86	0.67
Carboplatin Monotherapy IC_{75}	17.3 μM	34.41 μM
Combination Carboplatin IC_{75}	15.00 μM	N/A
Carboplatin CI at IC_{75}	0.96	N/A
Irinotecan Monotherapy IC_{50}	19.38 μM	1.65 μM
Combination Irinotecan IC_{50}	14.79 μM	0.24 μM
Irinotecan CI at IC_{50}	1.11	0.51
Irinotecan Monotherapy IC_{75}	39.82 μM	2.72 μM
Combination Irinotecan IC_{75}	27.4 μM	0.6 μM
Irinotecan CI at IC_{75}	0.79	0.56

Figure 5 *Continued.* **C,** a 72 h SRB growth assay was used in determining the extent of synergy between dasatinib and temozolomide. Glioma cells were treated with a fixed concentration of dasatinib (200 nmol/L) and the adjuvant concentration of temozolomide ranged from 5 to 250 μmol/L. Growth curves for dasatinib and temozolomide as monotherapies were compared with the combination growth effect to determine the CI for each concentration of temozolomide. Values < 1 indicate a synergistic drug relationship. The IC_{50} of temozolomide when combined with 200 nmol/L is significantly lower than temozolomide as a monotherapy, and the combination values for LN18, U87/EGFR, and U251 cells indicate a high degree of synergy. *Points,* mean of triplicate determinations from three independent experiments; *bars,* SD. Synergy values were determined using CalcuSyn. **D,** a 72 h growth curve was done using the SRB assay. U87/EGFR and U251 glioma cells were treated with a fixed dose of dasatinib (200 nmol/L) and increasing concentrations of carboplatin or irinotecan. Dose-effect curves were generated and the IC_{50} and IC_{75} values were calculated for the agent alone and in combination. The IC_{50} for dasatinib and irinotecan combination in U251 showed the greatest combination effect with an ~7-fold change in the effective IC_{50} of irinotecan alone. This combination appeared to be antagonistic (IC > 1) in U87 cells. Average of three independent experiments.

more sensitive to temozolomide than U251 cells; this may be due to the higher dose of temozolomide (50 μmol/L) needed to compensate for the relatively low dose of dasatinib. Nevertheless, an additive effect of the two drugs was revealed by increased acridine orange staining in both cell lines. The addition of 2.0 mmol/L 3-MA, a PI3K inhibitor that disrupts the formation of autophagosomes (37), after 24 h of dasatinib and temozolomide treatment

Published OnlineFirst February 3, 2009; DOI: 10.1158/1535-7163.MCT-08-0669

partially inhibited the increase in acridine orange staining. The same inhibition by 3-MA was seen when cells were treated for 72 h (data not shown).

To further investigate the possible autophagic effect, we analyzed cells treated with dasatinib and temozolomide for the presence and processing of microtubule-associated protein 1 LC3. LC3 is the first known mammalian protein that specifically associates with the autophagosomal membrane. An increase in expression of LC3-I and processing of LC3-I to the lower molecular weight form LC3-II is observed in autophagic (but not apoptotic) cells (38). GFP-LC3 has recently been shown to correlate with the induction of autophagy (38) and we used epifluorescence to further substantiate the idea that dasatinib induces glioma cell autophagy. In Fig. 5B, we show that both dasatinib and temozolomide are individually able to increase in the number and intensity of punctate LC3 fluorescence, representing autophagic vacuoles. Combination treatment with dasatinib and temozolomide further increased the number and intensity of punctuate LC3 fluorescence staining.

Western blotting of U87/EGFR cell lysates (Fig. 5B) showed an increase in LC3-I levels 24 and 48 h after treatment with dasatinib and temozolomide alone. There was an increase in processing of LC3-I to the lower molecular weight form LC3-II in U87/EGFR treated with dasatinib when comparing 24 with 48 h. Expression of LC3-I was elevated when dasatinib and temozolomide were applied to cells in combination for 48 h, more so than when cells were treated only with dasatinib or temozolomide. This enhancement of activity was confirmed by densitometry using Image J software (NIH; Fig. 5B). In contrast, U251 cells did not display a LC3-I signal increase until 48 h when treated with dasatinib alone, and temozolomide induced only a slight increase in LC3-I levels at 24 and 48 h. Regardless, LC3-I expression was more elevated when U251 cells were subjected to combination therapy than when treated individually with dasatinib or temozolomide. Conjointly, the expression of LC3 observed in both cell lines in response to treatment with dasatinib and temozolomide was successfully attenuated with the addition of 2.0 mmol/L 3-MA 24 h into treatment consistent with abrogation of autophagy. Several processes may have affected the accumulation of LC3-II in the U251 cell line experiments including the observation that LC3-II is degraded in cells undergoing autophagy (39) and that LC3-II may be converted back to LC3-I in late stages of autophagy (38). The combination of data obtained from acridine orange staining, LC3 epifluorescence, and LC3 Western blot analyses showing induction of autophagy and subsequent inhibition of autophagy after treatment with 3-MA emphasizes the ability of dasatinib to induce autophagy alone and in combination with temozolomide.

In view of the shared mechanism of action and the apparent additive effect at the molecular level between dasatinib and temozolomide, we examined the combination effect on cellular proliferation using a 72 h SRB growth assay (Fig. 5C). LN18, U251, and U87/EGFR cells were treated with a base concentration of 200 nmol/L dasatinib and varying concentrations of temozolomide ranging from 5 to 250 μmol/L. The result of the combination of dasatinib and temozolomide revealed synergistic cell growth inhibition ($P < 0.05$). Synergy was quantified by calculating a CI value for each data point, with values < 1 indicating synergism. With the exception of the 5 and 10 μmol/L combinations in LN18, all values obtained from the CI calculation indicated synergy. More dramatic, the IC_{50} of temozolomide in combination with 200 nmol/L dasatinib was markedly lower than the IC_{50} of temozolomide alone. The resultant IC_{50} values of temozolomide for LN18, U87/EGFR, and U251 were ~25.0, 50.0, and <5.0 μmol/L, respectively. These IC_{50} values represent a dramatic increase in sensitivity to temozolomide when combined with dasatinib than when used alone.

In addition to temozolomide, we tested the ability of two additional cytotoxic chemotherapy agents to augment the antiproliferative effect of dasatinib in glioma. The SRB assay was done using a fixed dose of dasatinib (200 nmol/L) in combination with increasing doses of carboplatin (2.5-20 μg/mL) and irinotecan (2.5-20 μg/mL), agents commonly used in patients with glioblastoma. Although there was a reduction in the IC_{50} and IC_{75} for both U87/EGFR and U251 cells lines for both combination treatments, only U251 cells treated with dasatinib and irinotecan showed a >5-fold increase in sensitivity compared with irinotecan treatment alone (Fig. 5D). Thus, combining dasatinib with chemotherapy agents exhibiting proapoptotic mechanisms of action (carboplatin and irinotecan) may be not as effective in inhibiting glioma proliferation compared with combining dasatinib and temozolomide.

Discussion

The invasive and proliferative nature of glioblastoma has been one of the impetuses for the testing of targeted therapy in this disease. Dasatinib (BMS-354825) is an orally bioavailable tyrosine kinase inhibitor, which shows exceptionally promiscuous inhibitive activity in multiple endothelial and solid tumors (7). In this report, we show that dasatinib is effective in glioblastoma by inhibiting tyrosine kinases such as SRC and EGFR, leading to the inhibition of proproliferative serine/threonine phosphorylation of AKT and rpS6, downstream indicators of PI3K and p70S6K activation, respectively. Additionally, we examined dasatinib sensitivity as a function of PTEN status and found that cells expressing functional PTEN were more sensitive than PTEN-deficient cells. *In vitro* proliferation and invasion of glioma cells were greatly reduced by treatment with dasatinib, with effective doses reaching low nanomolar, therapeutic concentrations. No apoptosis was observed; however, treatment with dasatinib induced considerable levels of autophagy in glioma cells. This type II programmed cell death was further magnified by combining dasatinib with low micromolar concentrations of temozolomide, resulting in a significant augmentation of

Published OnlineFirst February 3, 2009; DOI: 10.1158/1535-7163.MCT-08-0669

sensitivity to temozolomide. Less significant inhibition of cell proliferation was observed when dasatinib was combined with other cytotoxic chemotherapies such as carboplatin and irinotecan.

The PI3K pathway, which is up-regulated by PTEN deficiency and amplification of EGFR, has been heavily implicated in the genesis and progression of glioblastoma. AKT is a critical downstream mediator of PI3K, and phospho-PI3K and phospho-AKT levels correlate with more aggressive gliomas (40). A similar relationship among phospho-PI3K, p70S6K, and rpS6 has been described (37). High levels of these activated proteins have exhibited an inverse association with cleaved caspase-3 detection, intimating the suppression of apoptosis via PI3K. We found that AKT and rpS6 phosphorylation in U251 was decreased beginning at 8 and 4 h, respectively, when treated with the IC_{50} of dasatinib. This same inhibitory effect was observed when doses below the IC_{50} were employed for a period of 24 h, indicating the potency of dasatinib with respect to inhibiting the PI3K pathway. We also examined the activity of dasatinib against cells with wild-type and dysfunctional PTEN and in cells with a knockdown of PTEN (LN18 shPTEN). Although growth assays revealed that PTEN-competent cells were more sensitive to dasatinib than PTEN-deficient cells, the inhibitor continued to decrease activated SRC, AKT, and rpS6 in these cells at low concentrations. This effect was sustained even when cells were stimulated with EGF. Furthermore, activation of EGFR itself was curtailed, signifying either direct inhibition of EGFR phosphorylation or indirect inhibition through decreased cyclic SRC-EGFR phosphorylation (24). The increased sensitivity of LN18 and U87/EGFR PTEN cells may indicate an additive effect of PTEN phosphatase activity vis-à-vis AKT phosphorylation and indirect inhibition by dasatinib through SRC. It is also possible that PTEN is managing the activity of FAK, a known regulator of the cell cycle, whereas dasatinib simultaneously inhibits autophosphorylation of FAK through inhibition of SRC (41, 42).

The role of SRC in invasion and the targeting of SRC as a mechanism of inhibiting cellular invasion have been described in glioblastoma (18, 21, 22, 28, 43–45). Dasatinib abrogated Transwell migration *in vitro* in a dose-dependent manner at low nanomolar concentrations that effected little or no alteration in FAK activation, suggesting that this inhibition of cell migration is mainly due to SRC inhibition with additional augmentation by FAK inactivation at higher dasatinib concentrations. Our findings corroborate invasion studies conducted in various other malignancies (10, 12). Moreover, immunofluorescence studies indicated that dasatinib was able to attenuate colocalization of paxillin and actin to focal adhesions. Interestingly, PTEN-positive LN18 cells were slightly more resistant to dasatinib in the context of invasion than PTEN-defunct U251 cells, a finding that was intimated by both immunofluorescence and analysis of autophosphorylated FAK levels. This suggests that, although SRC is able to mediate invasion through FAK, most of the aforementioned PTEN-dasatinib additive effect may occur through the PI3K/AKT/p70S6K pathway in glioblastoma instead of through FAK.

Cell cycle analysis was done to assay for the presence of a sub-G_1 cell population. Very little G_1 arrest and no sub-G_1 population were observed in glioma cells treated with dasatinib. We confirmed the absence of apoptosis with Annexin V and terminal deoxynucleotidyl transferase-mediated dUTP nick-end labeling analyses. This finding is contrary to those of Johnson et al. (46) and Shor et al. (12), which detail the ability of dasatinib to induce apoptosis in squamous cell carcinoma and bone sarcoma cells, respectively. Intrigued, we investigated the possibility of dasatinib inducing type II programmed cell death or autophagy, a process through which intracellular vesicles sequester proteins and organelles for cellular recycling (47). By staining cells with acridine orange and examining LC3 epifluorescence and protein processing, we found that nanomolar concentrations of dasatinib significantly increase autophagic cell death in glioblastoma, an effect that has not been reported previously. Dasatinib-induced autophagy in glioma cells may offer a possible explanation for the increase in phospho-MAPK levels seen over the course of 48 h, because a similar increase in MAPK activity has been reported in HT-29 colon cancer cells (48). Unfortunately, many mechanisms of autophagy remain to be elucidated, truncating our understanding of the mechanisms by which dasatinib induces autophagy.

The alkylating agent temozolomide is known to induce G_2-M arrest and remains the front-line standard-of-care treatment for patients with glioblastoma. Temozolomide induces autophagy in glioma cells at doses >100 μmol/L (35). When combined with dasatinib, autophagy was induced at significantly lower doses of temozolomide. These two drugs were highly additive in combination: dasatinib significantly decreased the amount of temozolomide needed to achieve a 50% decrease in glioma cell proliferation and displayed an additive effect in combination with temozolomide with respect to induction of autophagy. Surprisingly, dasatinib combined with carboplatin or irinotecan did not lead to a significant decrease in cell proliferation or a dramatic decrease in the chemotherapy dose required to reach the IC_{50}, suggesting that perhaps using two agents that induce autophagy increases the therapeutic effect.

Advances in targeted molecular therapies are serving to more efficiently mitigate tumorigenic invasion, proliferation, and survival. A dasatinib monotherapy phase II trial for patients with recurrent glioblastoma (RTOG-0627) is ongoing, and we presented compelling data for the screening of tumors for SRC, EGFR, FAK, AKT, and PTEN expression to potentially predict response to this agent. Because some tumors and cell types have been shown to be refractory to temozolomide monotherapy, combination therapy with dasatinib may be a viable clinical option for resistant tumors (49, 50). Dasatinib, characterized here as an anti-invasive cytostatic agent in glioblastoma, may also be successfully combined with radiation therapy or anti-angiogenic therapy, which has been recently shown to

Published OnlineFirst February 3, 2009; DOI: 10.1158/1535-7163.MCT-08-0669

increase tumor invasion (51). We have initiated a study evaluating the efficacy of dasatinib in combination with temozolomide and radiation therapy in patients with newly diagnosed glioblastoma, and tumor screening will be critical in this study in determining the most important molecular predictors of outcome.

Disclosure of Potential Conflicts of Interest

No potential conflicts of interest were disclosed.

Acknowledgments

We thank Dr. William Bornmann for generously providing the dasatinib used in these studies.

References

1. Kleihues P, Louis DN, Scheithauer BW, et al. The WHO classification of tumors of the nervous system. J Neuropathol Exp Neurol 2002;61:215 – 25; discussion 226 – 9.

2. Louis DN, Ohgaki H, Wiestler OD, et al. The 2007 WHO classification of tumours of the central nervous system. Acta Neuropathol (Berl) 2007;114:97 – 109.

3. Puputti M, Tynninen O, Sihto H, et al. Amplification of KIT, PDGFRA, VEGFR2, and EGFR in gliomas. Mol Cancer Res 2006;4:927 – 34.

4. Stupp R, Mason WP, van den Bent MJ, et al. Radiotherapy plus concomitant and adjuvant temozolomide for glioblastoma. N Engl J Med 2005;352:987 – 96.

5. Davis FG, McCarthy BJ, Freels S, Kupelian V, Bondy ML. The conditional probability of survival of patients with primary malignant brain tumors: Surveillance, Epidemiology, and End Results (SEER) data. Cancer 1999;85:485 – 91.

6. Giese A, Bjerkvig R, Berens ME, Westphal M. Cost of migration: invasion of malignant gliomas and implications for treatment. J Clin Oncol 2003;21:1624 – 36.

7. Carter TA, Wodicka LM, Shah NP, et al. Inhibition of drug-resistant mutants of ABL, KIT, and EGF receptor kinases. Proc Natl Acad Sci U S A 2005;102:11011 – 6.

8. Doggrell SA. BMS-354825: a novel drug with potential for the treatment of imatinib-resistant chronic myeloid leukaemia. Expert Opin Investig Drugs 2005;14:89 – 91.

9. Lombardo LJ, Lee FY, Chen P, et al. Discovery of *N*-(2-chloro-6-methyl- phenyl)-2-(6-(4-(2-hydroxyethyl)- piperazin-1-yl)-2-methylpyrimidin-4- ylamino)thiazole-5-carboxamide (BMS-354825), a dual Src/Abl kinase inhibitor with potent antitumor activity in preclinical assays. J Med Chem 2004;47:6658 – 61.

10. Nam S, Kim D, Cheng JQ, et al. Action of the Src family kinase inhibitor, dasatinib (BMS-354825), on human prostate cancer cells. Cancer Res 2005;65:9185 – 9.

11. Chang YM, Kung HJ, Evans CP. Nonreceptor tyrosine kinases in prostate cancer. Neoplasia 2007;9:90 – 100.

12. Shor AC, Keschman EA, Lee FY, et al. Dasatinib inhibits migration and invasion in diverse human sarcoma cell lines and induces apoptosis in bone sarcoma cells dependent on SRC kinase for survival. Cancer Res 2007;67:2800 – 8.

13. Song L, Morris M, Bagui T, Lee FY, Jove R, Haura EB. Dasatinib (BMS-354825) selectively induces apoptosis in lung cancer cells dependent on epidermal growth factor receptor signaling for survival. Cancer Res 2006;66:5542 – 8.

14. Summy JM, Gallick GE. Src family kinases in tumor progression and metastasis. Cancer Metastasis Rev 2003;22:337 – 58.

15. Trevino JG, Summy JM, Lesslie DP, et al. Inhibition of SRC expression and activity inhibits tumor progression and metastasis of human pancreatic adenocarcinoma cells in an orthotopic nude mouse model. Am J Pathol 2006;168:962 – 72.

16. Courtneidge SA. Role of Src in signal transduction pathways. The Jubilee Lecture. Biochem Soc Trans 2002;30:11 – 7.

17. Frame MC. Src in cancer: deregulation and consequences for cell behaviour. Biochim Biophys Acta 2002;1602:114 – 30.

18. Irby RB, Yeatman TJ. Role of Src expression and activation in human cancer. Oncogene 2000;19:5636 – 42.

19. Sicheri F, Kuriyan J. Structures of Src-family tyrosine kinases. Curr Opin Struct Biol 1997;7:777 – 85.

20. Smart JE, Oppermann H, Czernilofsky AP, Purchio AF, Erikson RL, Bishop JM. Characterization of sites for tyrosine phosphorylation in the transforming protein of Rous sarcoma virus (pp60v-src) and its normal cellular homologue (pp60c-src). Proc Natl Acad Sci U S A 1981;78:6013 – 7.

21. Angers-Loustau A, Hering R, Werbowetski TE, Kaplan DR, Del Maestro RF. SRC regulates actin dynamics and invasion of malignant glial cells in three dimensions. Mol Cancer Res 2004;2:595 – 605.

22. Ding Q, Stewart J, Jr., Olman MA, Klobe MR, Gladson CL. The pattern of enhancement of Src kinase activity on platelet-derived growth factor stimulation of glioblastoma cells is affected by the integrin engaged. J Biol Chem 2003;278:39882 – 91.

23. Stettner MR, Wang W, Nabors LB, et al. Lyn kinase activity is the predominant cellular SRC kinase activity in glioblastoma tumor cells. Cancer Res 2005;65:5535 – 43.

24. Kassenbrock CK, Hunter S, Garl P, Johnson GL, Anderson SM. Inhibition of Src family kinases blocks epidermal growth factor (EGF)-induced activation of Akt, phosphorylation of c-Cbl, and ubiquitination of the EGF receptor. J Biol Chem 2002;277:24967 – 75.

25. Schaller MD, Hildebrand JD, Shannon JD, Fox JW, Vines RR, Parsons JT. Autophosphorylation of the focal adhesion kinase, pp125FAK, directs SH2-dependent binding of pp60src. Mol Cell Biol 1994;14:1680 – 8.

26. Testa JR, Bellacosa A. AKT plays a central role in tumorigenesis. Proc Natl Acad Sci U S A 2001;98:10983 – 5.

27. Vuori K, Hirai H, Aizawa S, Ruoslahti E. Introduction of p130cas signaling complex formation upon integrin-mediated cell adhesion: a role for Src family kinases. Mol Cell Biol 1996;16:2606 – 13.

28. Westhoff MA, Serrels B, Fincham VJ, Frame MC, Carragher NO. SRC-mediated phosphorylation of focal adhesion kinase couples actin and adhesion dynamics to survival signaling. Mol Cell Biol 2004;24:8113 – 33.

29. Conway AM, Rakhit S, Pyne S, Pyne NJ. Platelet-derived-growth-factor stimulation of the p42/p44 mitogen-activated protein kinase pathway in airway smooth muscle: role of pertussis-toxin-sensitive G-proteins, c-Src tyrosine kinases and phosphoinositide 3-kinase. Biochem J 1999;337:171 – 7.

30. Su B, Karin M. Mitogen-activated protein kinase cascades and regulation of gene expression. Curr Opin Immunol 1996;8:402 – 11.

31. Skehan P, Storeng R, Scudiero D, et al. New colorimetric cytotoxicity assay for anticancer-drug screening. J Natl Cancer Inst 1990;82:1107 – 12.

32. Chou TC, Talalay P. Quantitative analysis of dose-effect relationships: the combined effects of multiple drugs or enzyme inhibitors. Adv Enzyme Regul 1984;22:27 – 55.

33. Yeatman TJ. A renaissance for SRC. Nat Rev Cancer 2004;4:470 – 80.

34. Mellinghoff IK, Wang MY, Vivanco I, et al. Molecular determinants of the response of glioblastomas to EGFR kinase inhibitors. N Engl J Med 2005;353:2012 – 24.

35. Kanzawa T, Germano IM, Komata T, Ito H, Kondo Y, Kondo S. Role of autophagy in temozolomide-induced cytotoxicity for malignant glioma cells. Cell Death Differ 2004;11:448 – 57.

36. Paglin S, Hollister T, Delohery T, et al. A novel response of cancer cells to radiation involves autophagy and formation of acidic vesicles. Cancer Res 2001;61:439 – 44.

37. Kondo Y, Kanzawa T, Sawaya R, Kondo S. The role of autophagy in cancer development and response to therapy. Nat Rev Cancer 2005;5:726 – 34.

38. Kabeya Y, Mizushima N, Ueno T, et al. LC3, a mammalian homologue of yeast Apg8p, is localized in autophagosome membranes after processing. EMBO J 2000;19:5720 – 8.

39. Mizushima N, Yoshimori T. How to interpret LC3 immunoblotting. Autophagy 2007;3:542 – 5.

40. Chakravarti A, Zhai G, Suzuki Y, et al. The prognostic significance of phosphatidylinositol 3-kinase pathway activation in human gliomas. J Clin Oncol 2004;22:1926 – 33.

41. Tamura M, Gu J, Takino T, Yamada KM. Tumor suppressor PTEN

Published OnlineFirst February 3, 2009; DOI: 10.1158/1535-7163.MCT-08-0669

inhibition of cell invasion, migration, and growth: differential involvement of focal adhesion kinase and p130Cas. Cancer Res 1999;59:442–9.

42. Zhao JH, Reiske H, Guan JL. Regulation of the cell cycle by focal adhesion kinase. J Cell Biol 1998;143:1997–2008.

43. Park CM, Park MJ, Kwak HJ, et al. Ionizing radiation enhances matrix metalloproteinase-2 secretion and invasion of glioma cells through Src/epidermal growth factor receptor-mediated p38/Akt and phosphatidylinositol 3-kinase/Akt signaling pathways. Cancer Res 2006;66:8511–9.

44. Sloan KE, Stewart JK, Treloar AF, Matthews RT, Jay DG. CD155/PVR enhances glioma cell dispersal by regulating adhesion signaling and focal adhesion dynamics. Cancer Res 2005;65:10930–7.

45. Thomas SM, Brugge JS. Cellular functions regulated by Src family kinases. Annu Rev Cell Dev Biol 1997;13:513–609.

46. Johnson FM, Saigal B, Talpaz M, Donato NJ. Dasatinib (BMS-354825) tyrosine kinase inhibitor suppresses invasion and induces cell cycle arrest and apoptosis of head and neck squamous cell carcinoma and non-small cell lung cancer cells. Clin Cancer Res 2005;11:6924–32.

47. Kirkegaard K, Taylor MP, Jackson WT. Cellular autophagy: surrender, avoidance and subversion by microorganisms. Nat Rev Microbiol 2004;2:301–14.

48. Ogier-Denis E, Pattingre S, El Benna J, Codogno P. Erk1/2-dependent phosphorylation of Gα-interacting protein stimulates its GTPase accelerating activity and autophagy in human colon cancer cells. J Biol Chem 2000;275:39090–5.

49. Bocangel DB, Finkelstein S, Schold SC, Bhakat KK, Mitra S, Kokkinakis DM. Multifaceted resistance of gliomas to temozolomide. Clin Cancer Res 2002;8:2725–34.

50. Hirose Y, Berger MS, Pieper RO. p53 effects both the duration of G_2/M arrest and the fate of temozolomide-treated human glioblastoma cells. Cancer Res 2001;61:1957–63.

51. Norden AD, Young GS, Setayesh K, et al. Bevacizumab for recurrent malignant gliomas: efficacy, toxicity, and patterns of recurrence. Neurology 2008;70:779–87.

AACR American Association for Cancer Research

Molecular Cancer Therapeutics

Dasatinib-induced autophagy is enhanced in combination with temozolomide in glioma

Vanessa Milano, Yuji Piao, Tiffany LaFortune, et al.

Mol Cancer Ther 2009;8:394-406. Published OnlineFirst February 3, 2009.